Bound states in elastic waveguides

Dmitrii N. Maksimov and Almas F. Sadreev
Institute of Physics, Academy of Sciences, 660036 Krasnoyarsk, Russia and Department of Physics and Measurement Technology, Linköping University, SE-581 83 Linköping, Sweden

(Received 21 April 2006; published 6 July 2006)

We consider numerically the L-, T-, and X-shaped elastic waveguides with the Dirichlet boundary conditions for in-plane deformations (displacements) which obey the vectorial Navier-Cauchy equation. In the X-shaped waveguide we show the existence of a doubly degenerate bound state with frequency below the first symmetrical cutoff frequency, which belongs to the two-dimensional irreducible representation E of symmetry group C_{4v}. Moreover the next bound state is below the next antisymmetric cutoff frequency. This bound state belongs to the irreducible representation A_2. The T-shaped waveguide has only one bound state while the L-shaped one has no bound states.

DOI: 10.1103/PhysRevE.74.016201 PACS number(s): 46.40.Cd, 43.20.+g, 46.40.−f, 62.30.+d

I. INTRODUCTION

The question of the possible existence of bound states in special quantum waveguides was raised more than 20 years ago [1]. The simplest waveguide that supports a bound state is a bent one (curved waveguide). It is described by the two-dimensional Helmholtz equation

$$[\nabla^2 + k^2]\psi(x,y) = 0 \tag{1}$$

with Dirichlet boundary conditions (BCs). Such waveguides have no classically forbidden region (a classical particle could move freely through such a system), so the discovery by Lenz *et al.* [2] and by Exner and Šeba [3,4] that such a waveguide possesses a bound state was rather surprising. Exner and Seba [3,4] and Goldstone and Jaffe [5] then proved that at least one bound state exists for all two-dimensional waveguides of constant width, except waveguides of constant curvature, which have no bound states. Bound states were found also in more complicated structures: in the cross-terminal structure (the X-shaped waveguide) by Schult *et al.* [6] and Peeters [7], and in the T-shaped waveguide by Lin *et al.* [8].

Equation (1) exactly describes propagation of TE electromagnetic modes in waveguides [3,9,10], which allowed confirmation of the existence of the bound states experimentally [9,11]. Recently vectorial bound states were considered numerically in three-dimensional electromagnetic waveguides [12]. In the present paper we study the existence of bound states in L-, T-, and X-shaped elastic waveguides. In what follows, we shall assume that they consist of an isotropic material except for a case to be stipulated. To reduce the dimensionality of the problem, one can consider only waveguides of the form of a thin plate or an infinite rod with constant cross section. The displacements in the plate or the rod decouple then into two classes, the in-plane and the antiplane vibrations [13,14] (for plates, this is only true as long as the wavelength is much smaller than the thickness of the plate). The problem is thus reduced to two spatial dimensions. We will focus here on the in-plane waves for which the wave equation is still vectorial, which makes it more complex than the scalar Helmholtz equation (1). The wave field can be decomposed into two polarizations, which have different wave speeds. Furthermore, depending on the BCs imposed, different waves generally couple at the surface of body. These characteristics make vibrating solids more difficult to investigate than standard quantum or microwave transmission [15,16]. In particular the bound states have been considered rigorously only in a semi-infinite elastic stripe [17] for zero Poisson ratio. Because of the free boundary conditions these bound states are embedded in the continuum, i.e., they are the bound states in continuum first predicted by von Neumann and Wigner [18,19].

In what follows we will study the bound states in L-, T-, and X-shaped elastic waveguides by numerical methods.

II. THE STRAIGHT ELASTIC WAVEGUIDE

We consider the propagation of elastic waves in waveguides. The partial differential equation is the linear Navier-Cauchy equation [13,14]

$$\mu\nabla^2\mathbf{u} + (\lambda + \mu)\,\boldsymbol{\nabla}\,(\boldsymbol{\nabla}\mathbf{u}) + \rho\mathbf{u}\Omega^2 = 0 \tag{2}$$

where $\mathbf{u}(x,y)$ is the displacement field in the waveguide, λ,μ are the material-dependent Lamé coefficients, and ρ is the density. In what follows we will use dimensionless coordinates $x\to x/d$, $y\to y/d$ where d is half the width of the waveguide. Then Eq. (2) in terms of components of the elastic displacement $\mathbf{u}=(u,v)$ in the Cartesian coordinate system takes the following form:

$$c_l^2\frac{\partial^2 u}{\partial x^2} + c_t^2\frac{\partial^2 u}{\partial y^2} + (c_l^2 - c_t^2)\frac{\partial^2 v}{\partial x\,\partial y} + \omega^2 u = 0,$$

$$c_l^2\frac{\partial^2 v}{\partial y^2} + c_t^2\frac{\partial^2 v}{\partial x^2} + (c_l^2 - c_t^2)\frac{\partial^2 u}{\partial x\,\partial y} + \omega^2 v = 0, \tag{3}$$

where $\omega^2=\rho d^2\Omega^2/E$, $c_{l,t}$ are dimensionless wave velocities for thin plates

$$c_l^2 = \frac{1}{1-\sigma^2}, \quad c_t^2 = \frac{1}{2(1+\sigma)}, \tag{4}$$

and E and σ are the Young modules and the Poisson ratio, respectively. The Poisson ratio is the only parameter that affects the solution of Eq. (3). Formally Eq. (3) can be reduced to the Helmholtz equation (1) in the limit $c_l\to c_t$ or

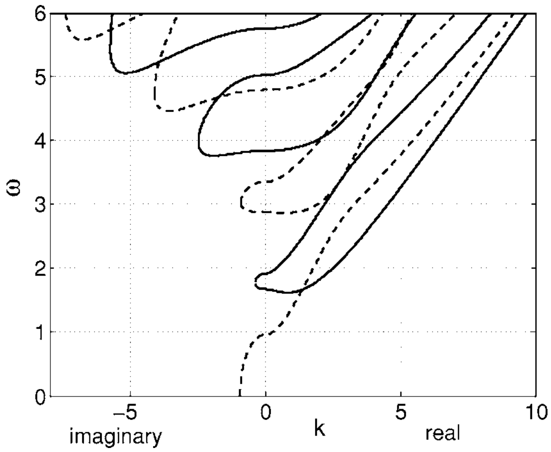

FIG. 1. Frequency spectra of an infinite straight waveguide with the Dirichlet BCs for real ($k>0$) and imaginary wave numbers ($k<0$). Solid lines are for the antisymmetric modes, dashed lines are for symmetric ones. $\sigma=0.345$ (aluminum).

$\sigma\to-1$. In fact the Poisson ratio ranges from 0 to 0.5 [13]. Therefore this limit is physically unreasonable. We direct the axis x along the straight waveguide, while the axis y is directed across the waveguide.

The general solution of the elastic equation (2) for straight waveguides is given, for example, in textbooks [14,20,21]. The solutions differ in parity relative to $y\to-y$. The symmetrical solution is

$$u=[ikA\cos(py)+qB\cos(qy)]e^{ikx},$$

$$v=[-pA\sin(py)+ikB\sin(qy)]e^{ikx}, \tag{5}$$

and the antisymmetrical solution has the form

$$u=[ikA\sin(py)-qB\sin(qy)]e^{ikx},$$

$$v=[pA\cos(py)-ikB\cos(qy)]e^{ikx} \tag{6}$$

where A and B are coefficients, one of which can be found from the BCs,

$$p^2=\frac{\omega^2}{c_l^2}-k^2, \quad q^2=\frac{\omega^2}{c_t^2}-k^2. \tag{7}$$

The dispersion equations for the free BCs are given in [14,20,21]. However, for the free BCs the eigenvalues of the elastic equation (3) ω^2 start from zero (zero cutoff frequency). This zero corresponds to free motion of the system as a whole. Therefore, in this case bound states with eigenfrequency below the propagation band do not exist. In what follows we consider waveguides with fixed BCs (the Dirichlet ones)

$$u(x,\pm 1)=0, \quad v(x,\pm 1)=0. \tag{8}$$

Then the dispersion equations take the following form:

$$\frac{pq}{k^2}=-\frac{\tan q}{\tan p}, \quad \frac{pq}{k^2}=-\frac{\tan p}{\tan q} \tag{9}$$

for the symmetric modes and the antisymmetric ones, respectively. The results of the numerical computation are shown in Figs. 1 and 2. Unlike the case of free BCs the frequency spectra of the elastic waveguides for the Dirichlet boundary conditions have nonzero cutoff frequencies. In particular, the lowest cutoff frequency for the first symmetric mode is

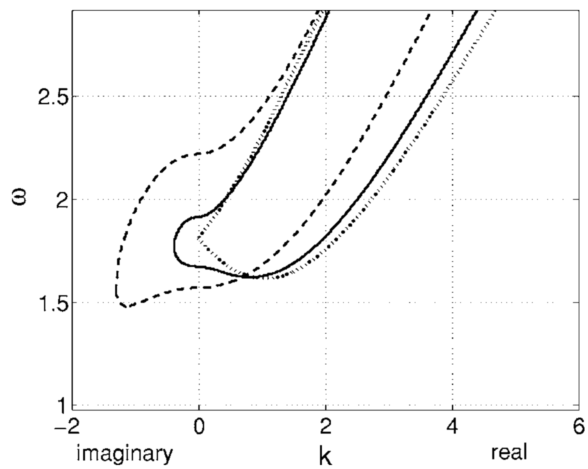

FIG. 2. The same as in Fig. 1. The frequency spectra for the lowest symmetric mode for three different values of the Poisson ration $\sigma=0$ (dashed line), 0.345 (solid line), and 0.5 (dotted line).

$$\omega_s=\frac{\pi}{2}c_l=\frac{\pi}{2}\sqrt{\frac{1}{2(1+\sigma)}}. \tag{10}$$

As shown in Fig. 2 the cutoff frequency of the antisymmetric mode is given by $k=0$ and equals

$$\omega_a=\pi c_t=\pi\sqrt{\frac{1}{1-\sigma^2}}, \tag{11}$$

provided that the Poisson ratio is small enough. If, however, the Poisson ratio exceeds 0.183, the minimum of the frequency spectrum is shifted to $k>0$. The cutoff frequency as dependent on the Poisson ratio is shown in Fig. 6 by solid lines.

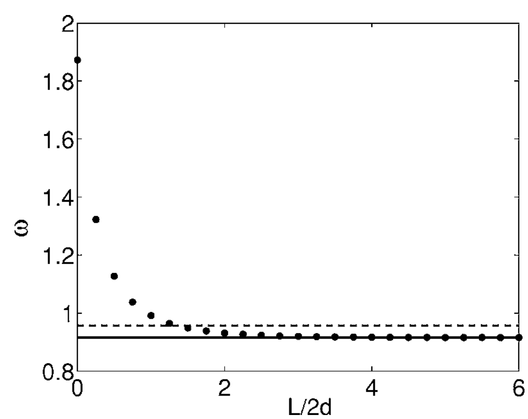

FIG. 3. The lowest eigenvalue of the closed X-shaped structure as dependent on the ratio $L/2d$ where L and $2d$ are the arm length and width, respectively. The lowest cutoff frequency (0.958) is shown by the dashed line; the asymptotic value of the frequency of the first bound state (0.916) is shown by the solid line.

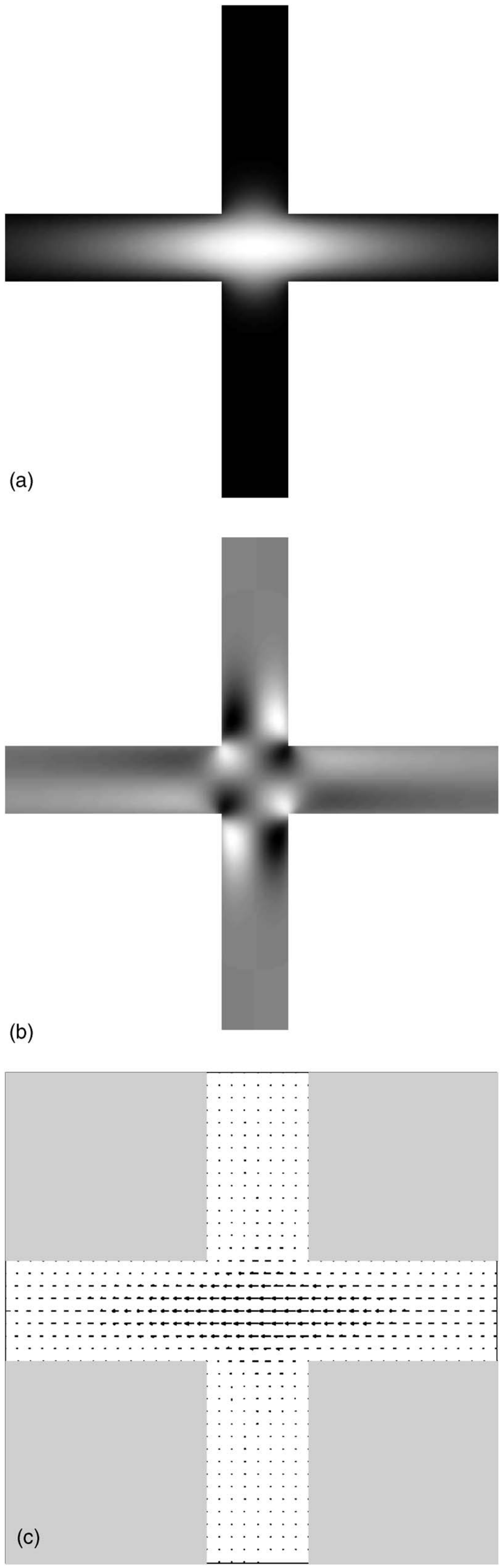

FIG. 4. Bound state patterns in X-shaped waveguide for the lowest frequency $\omega_1 = 0.916$. (a) shows solution for the deformation u, (b) for v, and (c) for the vectorial deformation $\mathbf{u} = (u, v)$. $\sigma = 0.345$ (aluminum plate).

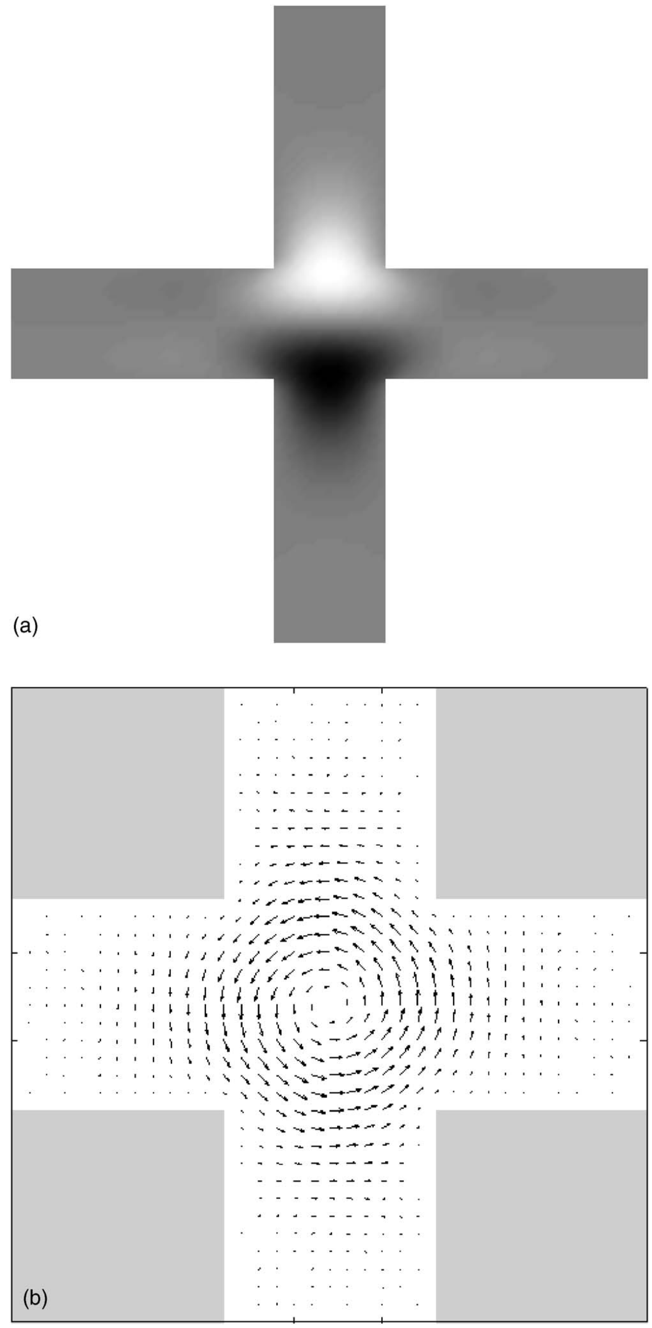

FIG. 5. Patterns of the next antisymmetric bound state in the X-shaped waveguide. (a) shows the solution for the deformation u. The solution for v can be easily obtained from the solution for u by a 90° rotation. (b) shows the vectorial deformation.

III. X-, T-, AND L-SHAPED WAVEGUIDES

There are many methods to find bound states [6,9,22,23]. Here we use the simpler but time-consuming method of brute-force numerical solution of Eq. (3) for the restricted structure as an eigenvalue problem with further asymptotic extension of the arm length L. Hence the final solution does not depend on the BCs at the end of the arm we imply the Dirichlet BCs there. To perform this procedure we approximate Eqs. (3) by finite-difference equations for

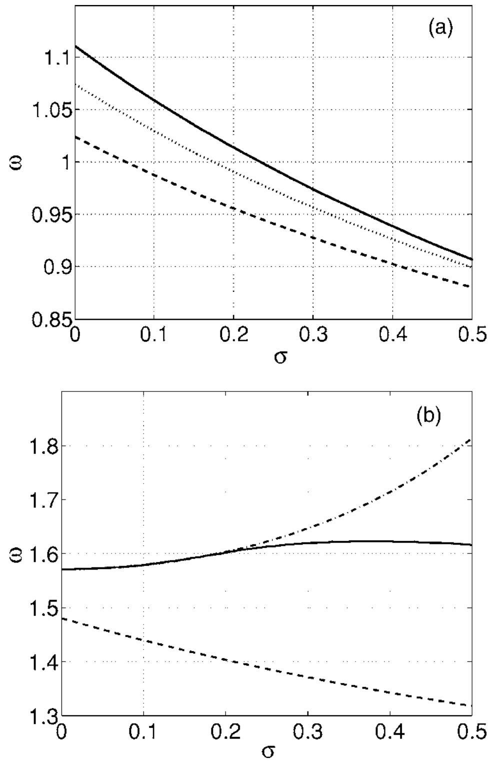

FIG. 6. The cutoff frequencies shown by solid lines and the frequency of the lowest symmetric bound state (a) and the first antisymmetric one (b) shown by dashed lines. The value of the frequency at $k=0$ given by formula (11) is plotted by the dash-dotted line. The dotted line shows the bound-state frequency in the T-shaped structure.

$u(x,y)\Rightarrow u(a_0 i, a_0 j)=u_j^i$, $v(x,y)\Rightarrow v(a_0 i, a_0 j)=v_j^i$:

$$c_l^2(u_{j+1}^i+u_{j-1}^i)+c_t^2(u_j^{i+1}+u_j^{i-1})-2(c_l^2+c_t^2)u_j^i+\frac{1}{4}(c_l^2-c_t^2)\times(v_{j+1}^{i+1}+v_{j-1}^{i-1}-v_{j-1}^{i+1}-v_{j+1}^{i-1})+a_0^2\omega^2 u_j^i=0,$$

$$c_t^2(v_{j+1}^i+v_{j-1}^i)+c_l^2(v_j^{i+1}+v_j^{i-1})-2(c_l^2+c_t^2)v_j^i+\frac{1}{4}(c_l^2-c_t^2)\times(u_{j+1}^{i+1}+u_{j-1}^{i-1}-u_{j-1}^{i+1}-u_{j+1}^{i-1})+a_0^2\omega^2 v_j^i=0. \quad (12)$$

The results of computation for the lowest eigenvalue of the aluminum X-shaped structure as dependent on the arm length L are shown in Fig. 3. One can see that the procedure of extension of the arm's length is converging rather fast and gives the frequency of the lowest bound state $\omega_1=0.916$, which is below the cutoff frequency of the first symmetric mode $\omega_s=0.958$ given by Eq. (10) for a specific value of the Poisson ratio $\sigma=0.345$ (aluminum). Figure 4 illustrates the bound state corresponding to the lowest eigenfrequency. Immediately one can see from Fig. 4(c) that there is a second degenerate bound state which differs from the former by 90° rotation of the vectorial deformation. Eigenfunctions of the cross structure are classified in five irreducible representations of the symmetry group C_{4v} [24], one of which, E, is two dimensional. Therefore the doubly degenerate bound states with frequency $\omega_1=0.916$ belong to the irreducible representation E. This result crucially differs from that in a quantum cross structure in which the lowest nondegenerate bound state forms the one-dimensional representation A_1 as can be seen from the solution shown by Schult *et al.* [6]. The degenerate solutions differ from each other only by rotation by 90°.

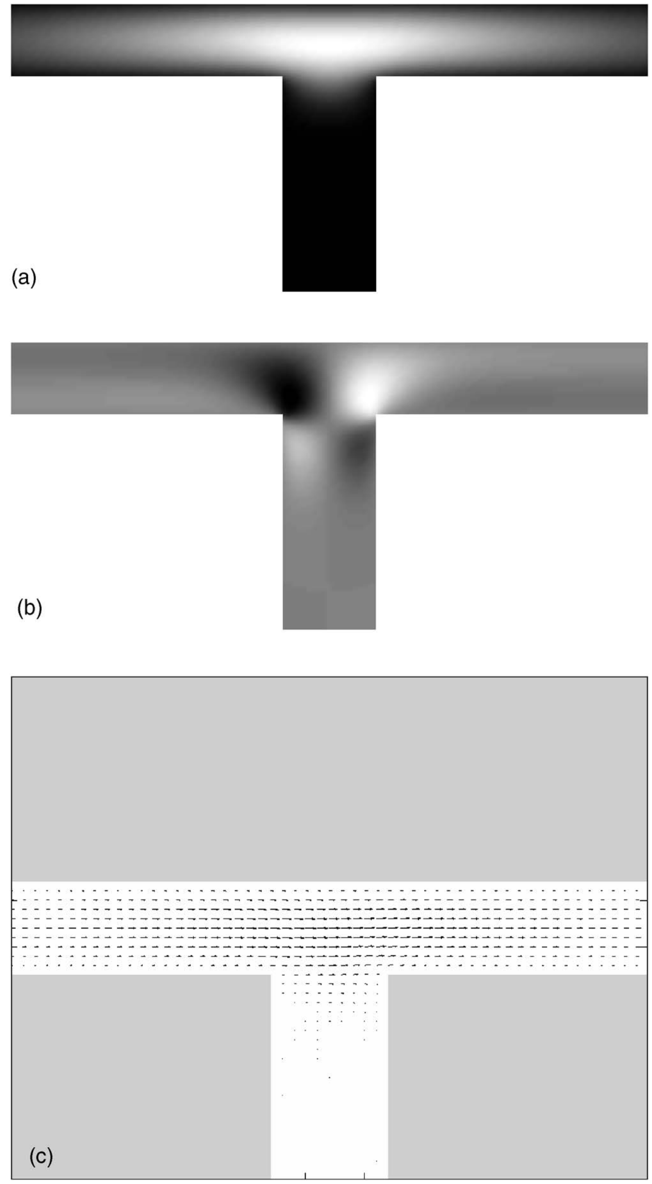

FIG. 7. Bound-state patterns in the T-shaped waveguide. (a) shows the solution for the deformation u, (b) for v, and (c) for the vectorial deformation $\mathbf{u}=(u,v)$. $\omega=0.943$, $\sigma=0.345$ (aluminum plate).

Computation reveals also the next bound state with frequency $\omega_2=1.356$ which is below the cutoff frequency ω_a of the first antisymmetric mode shown in Fig. 2. This solution is nondegenerate and belongs to the irreducible representation A_2 as seen from Fig. 5(b). This bound state again differs from the result for the quantum cross structure in which the next bound state forms the irreducible representation B_2. Any bound states that belong to different irreducible representa-

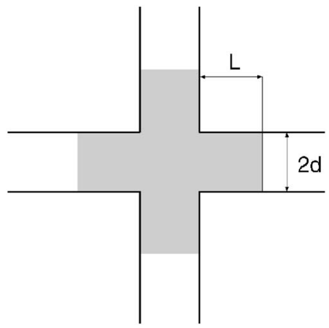

FIG. 8. The X-shaped waveguide fabricated of two different materials. The inner material (dark) has a density exceeding the density of the arms shown in white.

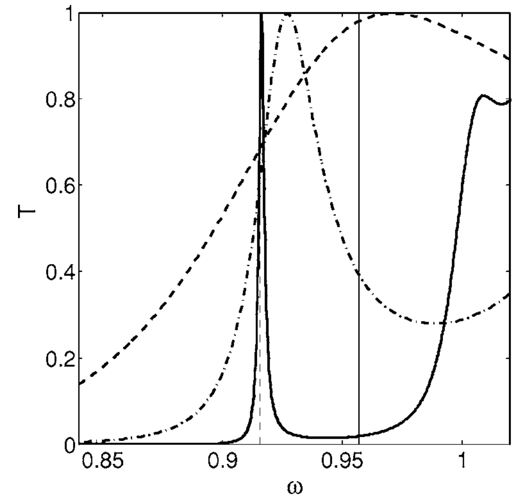

FIG. 9. Calculated elastic power transmission in the X-shaped waveguide fabricated from two different elastic materials as shown in Fig. 8. Dashed vertical line shows the bound-state frequency given in Fig. 4. Thin solid line shows the cutoff frequency of the inner cross structure. With an extension of the heavier material the resonance induced by the bound state becomes sharper: dashed line for $L/2d=1$, dotted-dashed line for $L/2d=2$, and solid line for $L/2d=4$.

tions of the symmetry group C_{4v} were not found in our computations. The frequency of the bound states depends on the elastic material via the Poisson ratio σ ranging from 0 to 0.5 [13]. However, as computation shows, both bound states exist irrespective of the Poisson ratio as illustrated in Fig. 6. Next, our computations reveal one bound state in the T-shaped waveguide shown in Fig. 7 but we did not find a bound state in the L-shaped waveguide, in contrast to the quantum case [2,3]. The dependence of the bound-state frequency on σ is shown in Fig. 6(a).

The bound-state frequencies can be detected by resonance peaks in elastic power transmission provided that waveguides of different material are attached to the structures considered above [25]. We took waveguides of material with lower density compared to the material of the inner region as shown in Fig. 8. Specifically the ratio of densities was taken as 0.8. This construction has the cutoff frequency of the attached waveguides below the bound-state frequency. As a result this frequency becomes accessible for propagating modes in the waveguides and gives rise to typical resonant peaks in the transmission as shown in Fig. 9. The resonance width decreases with extension of the inner material.

IV. CONCLUSIONS

Numerical solution of the two-dimensional Navier-Cauchy equation (3) describing the vectorial vibrations shows different bound states in waveguides of the form of a thin plate, provided that the Dirichlet BCs are adopted. The X-shaped waveguide is the richest one, in which we reveal two types of bound states as in the quantum waveguide [6]. However, in the elastic X-shaped waveguide the bound state with the lowest frequency of vibrations is doubly degenerate and belongs to the two-dimensional irreducible representation E of symmetry group C_{4v}. The next bound state forms the irreducible representation A_2. The T-shaped waveguide has only one bound state while the L-shaped one has no bound states unlike the quantum case. We have shown also that these bound states exist irrespective of the choice of the Poisson ratio σ, although the frequencies of the bound states depend on σ.

Similar to the approach of Berggren and Ji [25], we considered the elastic power transmission through an X-shaped waveguide fabricated of two elastic materials with different mass densities as shown in Fig. 8, and showed resonant peaks caused by the bound state in the inner material. We have to note that although the Dirichlet BCs cannot be achieved completely, they can be satisfied approximately if an elastic waveguide is fixed at the boundaries with a material with rigidity substantially exceeding the rigidity of the waveguide.

ACKNOWLEDGMENTS

We greatly appreciate discussions with Evgeny N. Bulgakov. This work has been supported by RFBR Grant No. 05-02-97713 "Enisey" and by a Swedish Royal Academy of Sciences grant.

[1] H. Sakaki, in *Proceedings of the International Symposium on Foundations of Quantum Mechanics in the Light of New Technology*, edited by S. Kamefuchi *et al.* (Physical Society of Japan, Tokyo, 1984), pp. 94–110.
[2] F. Lenz, J. T. Londergan, E. J. Moniz, R. Rosenfelder, M. Stingl, and K. Yazaki, Ann. Phys. (N.Y.) **170**, 65 (1986).
[3] P. Exner and P. Šeba, J. Math. Phys. **30**, 2574 (1989).
[4] P. Exner, P. Šeba, and P. Štoviček, Czech. J. Phys., Sect. B **39**, 1181 (1989).
[5] J. Goldstone and R. L. Jaffe, Phys. Rev. B **45**, 14100 (1992).

[6] R. L. Schult, D. G. Ravenhall, and H. W. Wyld, Phys. Rev. B **39**, 5476 (1989).
[7] F. M. Peeters, Superlattices Microstruct. **6**, 217 (1989).
[8] Y.-K. Lin, Y.-N. Chen, and D.-S. Chuu, Phys. Rev. B **64**, 193316 (2001).
[9] J. P. Carini, J. T. Londergan, K. Mullen, and D. P. Murdock, Phys. Rev. B **48**, 4503 (1993).
[10] H.-J. Stöckmann, *Quantum Chaos: An Introduction* (Cambridge University Press, Cambridge, U.K., 1999).
[11] J. P. Carini, J. T. Londergan, K. Mullen, and D. P. Murdock, Phys. Rev. B **46**, 15538 (1992); J. P. Carini, J. T. Londergan, D. P. Murdock, D. Trinkle, and C. S. Yung, *ibid.* **55**, 9842 (1997).
[12] G. Annino, H. Yashiro, M. Cassettari, and M. Martinelli, Phys. Rev. B **73**, 125308 (2006).
[13] L. D. Landau and E. M. Lifshitz, *Theory of Elasticity* (Pergamon, Oxford, 1959).
[14] J. D. Achenbach, *Wave Propagation in Elastic Solids* (North-Holland Publishing Company, Amsterdam, 1973).
[15] P. Bertelsen, C. Ellegaard, and E. Hugues, Eur. Phys. J. B **15**, 87 (2000).
[16] N. Sondergaard and G. Tanner, Phys. Rev. E **66**, 066211 (2002).
[17] I. Roitberg, D. Vassiliev, and T. Weidl, Q. J. Mech. Appl. Math. **51**, 11 (1998).
[18] J. von Neumann and E. Wigner, Phys. Z. **30**, 465 (1929).
[19] F. H. Stillinger and D. R. Herrick, Phys. Rev. A **11**, 446 (1975).
[20] R. D. Mindlin, in *Structural Mechanics*, edited J. N. Goodier and N. J. Holf (Pergamon Press, New York, 1960).
[21] J. Miklowitz, *Elastic Waves and Waveguides* (North-Holland Publishing Company, Amsterdam, 1978).
[22] Y. Avishai, D. Bessis, B. G. Giraud, and G. Mantica, Phys. Rev. B **44**, 8028 (1991).
[23] E. N. Bulgakov, P. Exner, K. N. Pichugin, and A. F. Sadreev, Phys. Rev. B **66**, 155109 (2002).
[24] L. D. Landau and E. M. Lifshitz, *Quantum Mechanics* (Pergamon Press, New York, 1965).
[25] K.-F. Berggren and Z.-L. Ji, Phys. Rev. B **43**, 4760 (1991).